Water-Floatable Organosilica Particles for TiO_2 Photocatalysis

Yusuke Maki,[a] Yusuke Ide,[b] and Tomohiko Okada,[a]*

[a] Department of Chemistry and Material Engineering, Faculty of Engineering, Shinshu University, Wakasato 4-17-1, Nagano 380-8553, Japan

[b] International Center for Materials Nanoarchitectonics (MANA), National Institute for Materials Science (NIMS), 1-1 Namiki, Tsukuba 305-0044, Japan

Corresponding author: tomohiko@shinshu-u.ac.jp (T. Okada)

Keywords: Floating photocatalyst, Organosilica, Anatase, 3-Aminopropyltrimethoxysilane, Titanium (IV) oxysulfate sulfuric acid hydrate

ABSTRACT. A water-floatable TiO_2 photocatalyst support was successfully produced from organosilica via sol-gel reactions of organosilanes (octyl- and methyl-silyl trichlorides and 3-aminopropyltrimethoxysilane). 3-Aminopropyltrimethoxysilane in silane coupling agents was shown to have an important role in depositing highly dispersed TiO_2 nanocrystals onto organosilica particles. Calcination of the as-made sample at 400 °C in an airflow resulted in the loss of octyl- and 3-aminopropyl groups, modifying polymethylsiloxane while maintaining water floatability. Calcination led to an increase in the specific surface area from 88 to 230 m^2/g and the growth of anatase crystallites. Floatability was not observed when the as-made sample was calcined at 600 °C, showing that methyl groups acted as surfactants at the air–water interface. Formic acid in water was catalytically oxidized over the water-floatable sample upon irradiation by a solar simulator. The evolved CO_2 became saturated when the surface of the aqueous solution was filled with the floating particles. We demonstrated the importance of the floating photocatalyst with respect to the efficiency of light receipt and facile recovery from liquid media.

1. Introduction

Structural and morphological modification of titanium dioxides (TiO_2) has been an important task with respect to the enhancement of photocatalytic activity and usability. Effective contact of light with the photocatalyst plays a key role in achieving such an enhancement. Hybridization of TiO_2 with different solids is a solution to this issue because this strategy has numerous advantages, such as improved affinity toward reactants, increased surface areas, prevention of TiO_2 aggregation, and facile separation from liquid media [1-3]. On the other hand, efforts have also been made to produce "phase boundary catalysts." This type of photocatalyst is active at liquid–liquid [4,5] and gas–liquid interfaces. The latter concept involves floating photocatalysts for use at an air–water interface, where TiO_2 hybrids float on the liquid surface [6-16]. It has been indicated that this system is advantageous with regard to facile recovery from liquid media and the efficient receipt of light at an air–water interface in order to decompose contaminants in/on water. Several floatable catalyst supports have been proposed, such as graphite [6], organic polymers [7-10] and minerals with low bulk density (e.g., vermiculite [11], perlite [12], and fly-ash[13,14]). Hollow glass microspherical particles have also been reported to show a possible application in this floating system [15,16].

Silica-based porous materials are candidates for such floating photocatalyst supports because of their large surface area and variable structure/morphology. Surface modification of porous silicas using covalent attachment has been investigated to impart reaction selectivity [17,18]. Sol–gel reactions of appropriate organic moieties with silane coupling agents are a useful synthetic strategy for achieving one-pot fabrication of organosilicas without a post modification process. In addition to structural versatility, the formation of hollow shapes in the silica-based system [19,20] is a characteristic that exemplifies their morphological flexibility

[21]. This is worth noting as a merit of using hollow particles in a floating system; however, a thinner shell would be required. We recently developed porous cup-shaped hollow polymethylsiloxane particles with nano-order thickness (20–120 nm) [22]. The synthetic approach was based on the deposition of a polyalkylsiloxane shell on water droplets in a water-in-oil (W/O) emulsion through the sol-gel reactions of octyl- and methyl-trichlorosilanes, followed by calcination to decompose the octyl groups [23-25]. Using sol-gel reactions, appropriate surface modification by selection of silane coupling agents is possible to firmly immobilize TiO_2 without using any bulkier additives such as organic polymers.

Here, we report the development of floating photocatalyst particles by dispersing TiO_2 nanocrystals onto organosilica particles. The organosilicas were prepared by cooperative polycondensation of hydrolyzed organosilyl groups, including 3-aminopropyltrimethoxysilane, on water droplets dispersed in an organic solvent. Titanium (IV) oxysulfate-sulfuric acid hydrate was adopted [26-28] as the TiO_2 precursor. A slow rate of the hydrolysis gives titanium oxyhydroxide, $TiO(OH)_2$, giving anatase with lower crystallinity [28]. Good dispersion of TiO_2 is expected via acid–base interactions with amino groups on the resulting organosilica particles. Photo-oxidation of formic acid in water by irradiation using a solar simulator was examined as a test reaction. The mechanism of the TiO_2 dispersion, the origin of the water floatability, and the photocatalytic activity will be discussed in this paper.

2. Experimental

2.1. Materials

Isooctane (2,2,4-trimethylpentane), 3-aminopropyltrimethoxysilane (APTMS), titanium (IV) tetraisopropoxide, ethanol (99.5%), and formic acid were purchased from Wako Pure Chemical Ind. Co., Ltd. Octyltrichlorosilane (OTCS) and titanium (IV) oxysulfate-sulfuric acid hydrate ($TiOSO_4 \cdot xH_2SO_4 \cdot xH_2O$) were purchased from Aldrich Chemical Co., Ltd. Methyltrichlorosilane (MTCS) was obtained from Shin-Etsu Chemical Ind. Co., Ltd. These materials were used as received. AEROXIDE TiO_2 P25 (Nippon Aerosil) was used as a reference photocatalyst.

2.2. Preparation of organosilica particles containing amino groups

A W/O emulsion was prepared by mixing 0.75 mL of water and 2.4 mmol of OTCS dissolved in 50 mL of isooctane, followed by ultrasonic agitation (45 kHz) for 5 min. Then, 1.6 mmol of MTCS dissolved in 10 mL of isooctane was poured into the W/O emulsion under magnetic stirring. Thirty minutes after MTCS addition, APTMS (0.2 mmol) in 10 mL of isooctane was added to the mixture, accompanied by continuous stirring at room temperature, which was continued for 3 h. During stirring, water-saturated air was continuously supplied (0.11 L min^{-1}) to remove evolved HCl and to accelerate the hydrolysis and polymerization of the organosilanes. The resulting precipitate was separated by centrifugation, washed thoroughly with isooctane, and then dried at 50 °C for 24 h. This dried sample is denoted as S_N-50, hereafter. Another sample, which does not contain amino groups, was prepared using the same procedure, except that 1.8 mmol MTCS was added without APTMS (the resulting sample is denoted as S_0-50).

2.3. Hybridization of titanium oxide with organosilica particles

A titanium oxide precursor was prepared by mixing $TiOSO_4 \cdot xH_2SO_4 \cdot xH_2O$, ethanol and water, which were stirred for 3 h in an ice box at a $TiOSO_4$:H_2O:ethanol molar ratio of 1:850:240. The dried sample (S_N-50 or S_0-50) was added to the titanium oxide precursor at a TiO_2:organosilica weight ratio of 1:1. The mixture was then transferred to a Teflon-lined autoclave, heated to 80 °C, and kept at this temperature for 24 h. The autoclave was rotated at 11 rpm during heat treatment using a hydrothermal synthesis reactor unit (Hiro Company). After centrifugation, floating particles at the air-solution interface were collected to afford products that are denoted as TiO_2/S_0-50 or TiO_2/S_N-50. TiO_2/S_N-50 was calcined at 400 and 600 °C using a tubular furnace with an air flow (50 mL/min) for 3 h and the calcined products thus obtained are designated as TiO_2/S_N-400 and TiO_2/S_N-600, respectively. Furthermore, titanium oxide (TiO_2) particles with no support were also prepared using the same procedure for the following photocatalytic activity test.

2.4. Photocatalytic activity test

Photocatalytic oxidation reactions were conducted by irradiation with a solar simulator (San-Ei Electric Co., Ltd.) in a closed stainless steel container equipped with a 75 mL Pyrex glass vessel containing 15–60 mg catalyst and 5 mL of an O_2-saturated solution of 5% aqueous formic acid. The container was placed ca. 30 cm away from a simulated solar light source (1000 Wm^{-2}) to irradiate the mixture for 30 min at a temperature of 42 °C. Under this condition, CO_2 evolved linearly with irradiation time by at least 90 min. The amount of evolved CO_2 was determined using a Shimadzu GC-2010 plus gas chromatograph~~er~~ equipped with a dielectric barrier discharge ionization (BID) detector.

2.5. Equipment

X-Ray powder diffraction (XRD) patterns were obtained using a Rigaku RINT 2200 V/PC diffractometer (monochromatic Cu Kα radiation) operated at 20 mA and 40 kV. Thermogravimetric–differential thermal analysis (TG–DTA) curves were recorded on a Rigaku TG8120 instrument at a heating rate of 10 °C/min using α-alumina as the standard material. Nitrogen adsorption-desorption isotherms were measured at −196 °C on a Belsorp–mini (MicrotracBEL, Inc.). Before the adsorption experiment, the samples were heat treated at 120 °C under reduced pressure. Scanning electron micrographic (SEM) images were captured on a Hitachi S-4100 field-emission scanning electron microscope (operated at 15 kV) after applying a platinum plasma coating to the samples. Energy dispersive X-ray (EDX) elemental maps were obtained on a HORIBA EMAX–5770Q EDX spectrometer (accelerating voltage 15 kV). Transmission electron micrographic (TEM) observations were conducted using a Hitachi HD2300A scanning transmission electron microscope, which has an accelerating voltage of 200 kV. Fourier-transform infrared (FT-IR) spectra were obtained using a JASCO FT/IR–4200 spectrophotometer. Solid-state ^{13}C-cross-polarization/magic angle spinning (CP/MAS) nuclear magnetic resonance (NMR) spectra were measured on a Bruker ASCEND 500 spectrometer at a resonance frequency of 125.76 MHz. Glycine was used as the external standard.

3. Results and Discussion

3.1. Immobilization of TiO_2 nanoparticles on the organosilicas

SEM and TEM images of the products obtained by reactions of titanium (IV) oxysulfate with organosilicas (S_N-50 and S_0-50: the TiO_2 supports) are shown in Fig. 1. The organosilica particles are basically cup-shaped with sizes of 3–10 μm, irrespective of APTMS addition. It has

been reported that cup-shaped particles form as a result of deformation of hollow spheres; this is achieved using the W/O emulsion technique with smaller amounts of OTCS and MTCS [24]. While no particles were observed on the surface of S_0-50 (Fig. 1a), there are fine particles with sizes of several tens of nm on the surfaces of S_N-50 (Fig.s 1b and 1c). EDX elemental maps (Si and Ti) revealed that the fine particles are TiO_2 (The elemental mapping images are shown in the Supplementary Data, Fig. S1). FT-IR spectrum of S_N-50, shown in Fig. 2a, exhibited an absorption bands assigned to bending vibrations of N–H bonds [29,30] at around 1550 and 1530 cm^{-1}. These bands shifted to a higher wavelength region (around 1560 and 1540 cm^{-1}, respectively, Fig. 2b) by TiO_2 hybridization, suggesting that amino groups interacted with TiO_2. We speculate that the interactions comprise acid–base characteristics between nitrogen of the amino groups and a distorted five-coordinate Ti^{4+} acting as the Lewis acidic site [28,31]. The base characteristic of the bare amino groups would involve a spectral shift due to bending vibration of the adsorbed water molecules to 1590 cm^{-1} (Fig. 2a). Hence, it is clearly shown that APTMS, when included in the organosilica fabrication, is beneficial to the dispersion of TiO_2 on the surface. When titanium (IV) tetraisopropoxide, rather than titanium (IV) oxysulfate, was used as the TiO_2 source, we failed to immobilize TiO_2 particles on the surface of S_N-50 (SEM images and EDX elemental Si and Ti maps are shown in the Supplementary Data, Fig. S2). We assume that this phase separation is due to differences in the rates of the hydrolysis and polycondensation reactions of the TiO_2 precursors used. Because the rate was quite high for titanium (IV) tetraisopropoxide, large TiO_2 particles with small Ti–OH content would form. On the other hand, owing to the slower rate for titanium (IV) oxysulfate, acid–base interactions with amino groups in S_N-50 are thought to play an effective role in the observed high dispersion of TiO_2.

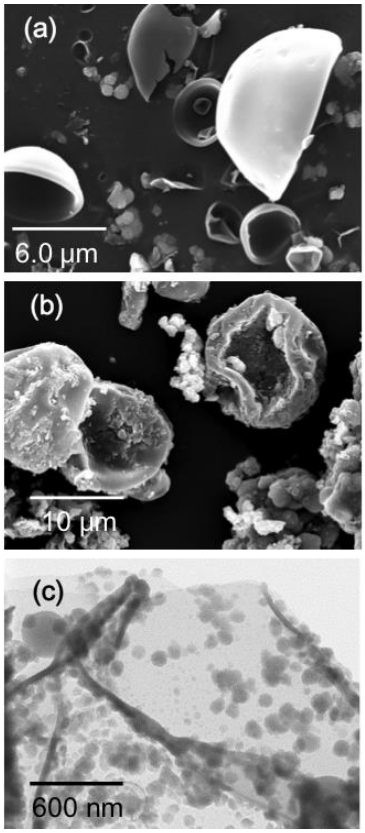

Fig. 1. SEM images of (a) TiO_2/S_0-50, (b) TiO_2/S_N-50 particles and (c) TEM image of a typical TiO_2/S_N-50 particle.

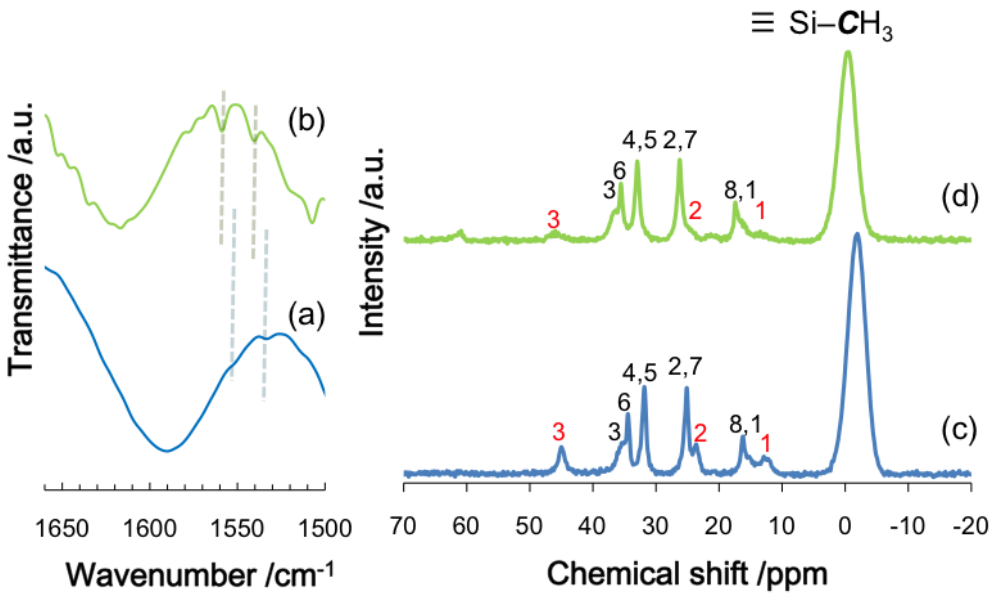

Fig. 2. FT-IR spectra of (a) S_N-50, (b) TiO_2/S_N-50, and solid-state ^{13}C-CP/MAS NMR spectra of (c) S_N-50 and (d) TiO_2/S_N-50.

Solid-state ^{13}C-CP/MAS NMR spectra of S_N-50 and TiO_2/S_N-50 are shown in Fig.s 2c and 2d, respectively. By comparing with those reported in literature [32], signals 1–8 in black and 1–3 in red can be attributed to the bonding of octyl and 3-aminopropyl groups, respectively, to each silicon atom. The signal at ~0 ppm can be assigned to C–Si bonds where methyl groups have bonded to silicon atoms. Thus, the as-made S_N-50 and TiO_2/S_N-50 are shown to include methyl, propyl, and octyl groups bonded to Si.

TG–DTA curves of S_N-50 (Fig. 3A) exhibit a weak exothermic peak in the temperature range of 200–400 °C in the DTA curve, and this peak is accompanied by mass loss (ca. 15 mass%) in the corresponding TG curve. In addition, a strong exothermic peak in the range of 450–600 °C with a mass loss of ca. 15% was observed in the TG–DTA curves. Upon calcination

of TiO_2/S_N-50 at 400 °C, the FT-IR absorption bands assigned to C–H bonds remained at 2960 and 2850 cm^{-1} (the spectrum is shown in Fig. 3B-a). Only the methyl groups bonded to a silicon atom (~0 ppm) remained in the ^{13}C-CP/MAS NMR spectrum (Fig. 3C), suggesting that the octyl and the 3-aminopropyl groups in the TiO_2/S_N-50 were oxidatively decomposed to afford a TiO_2–polymethylsiloxane hybrid by calcination at 400 °C (the product is denoted as TiO_2/S_N-400). In addition, disappearance of the FT-IR absorption bands assigned to C–H bonds (Fig. 3B-b) upon calcination at 600 °C suggests transformation to TiO_2–SiO_2 hybrid particles (denoted as TiO_2/S_N-600). TEM images of TiO_2/S_N-400 and TiO_2/S_N-600 (Fig. 3D) show agglomerated TiO_2 nanoparticles on both supports. The TiO_2 nanoparticles are anatase crystals, as evidenced in the XRD patterns (Fig. 3E). The diffraction peaks ascribed to anatase were relatively sharp compared with those for TiO_2/S_N-50. It is thought that the crystallinity increased as a result of calcination. The crystallite size in TiO_2/S_N-400 was estimated from the (101) plane at 2θ = 25.3 degree (Cu Kα) using Scherrer's equation to be ca. 5 nm. After calcination at 600 °C, the size increased to ca. 9 nm.

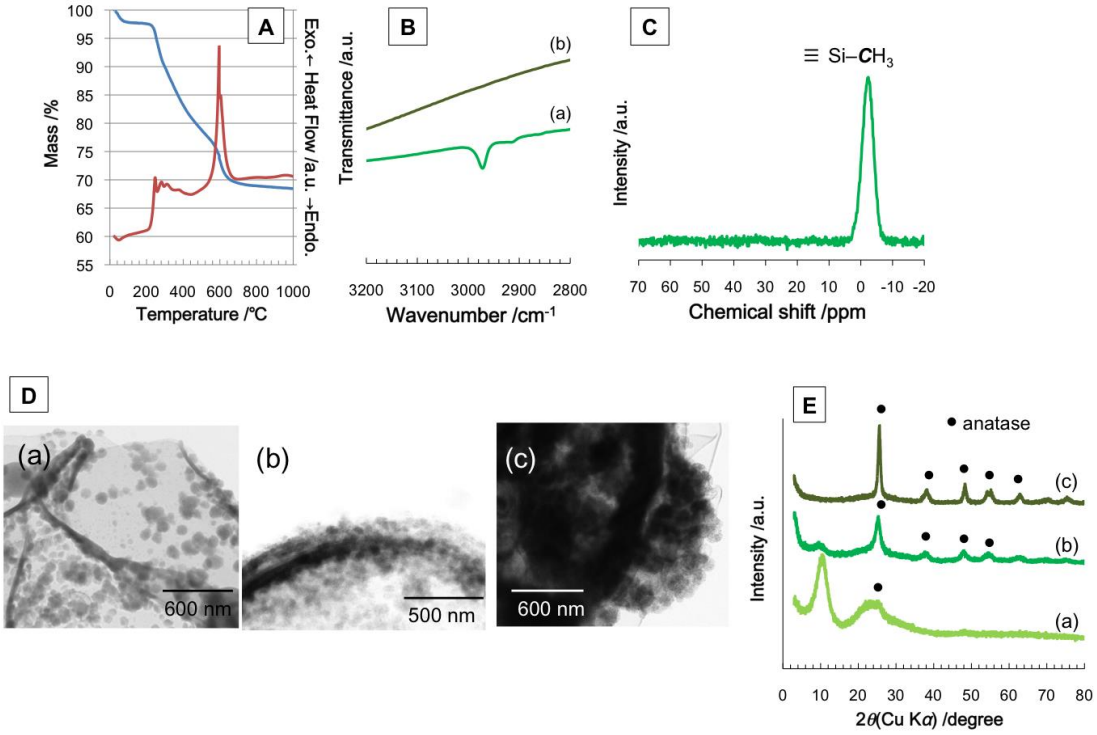

Fig. 3. (A) TG–DTA curves of S_N-50; (B) FT-IR spectra of (a) TiO_2/S_N-400, (b) TiO_2/S_N-600; (C) solid-state ^{13}C-CP/MAS NMR spectrum of TiO_2/S_N-400; (D) TEM images of (a) TiO_2/S_N-50, (b) TiO_2/S_N-400, and (c) TiO_2/S_N-600; (E) XRD patterns of (a) TiO_2/S_N-50, (b) TiO_2/S_N-400, and (c) TiO_2/S_N-600.

Specific surface areas, which were determined by Bruanauer–Emmett–Teller (BET) plots of the N_2 adsorption isotherms, of the three TiO_2/S_N samples together with that of S_N-50 are listed in Table 1. The BET surface area of S_N-50 was 123 m^2/g, indicating a microporous solid. The surface area of TiO_2/S_N-50 (98 m^2/g) increased to 230 m^2/g after calcination at 400 °C, while subsequent calcination at 600 °C decreased the surface area to 88 m^2/g. According to previous studies [24,25,27], the calcination temperature determines the microporosity;

calcination at 400 °C removes alkyl groups (*n* of C*n* >1) buried in the micropores of polymethylsiloxane. Further calcination results in conversion to dense silica with a low surface area (<40 m^2/g). Owing to the very fine TiO_2 particles, these TiO_2/S_N hybrids can be recognized as microporous photocatalysts. Molar Ti:Si ratios determined by EDX analyses were approximately 1:2 in the TiO_2/S_N samples, as shown in Table 1.

Table 1. BET specific surface area, chemical composition and crystallite size of anatase in the present samples.

Sample	BET specific surface area (m^2/g)	molar ratio		mass ratio		crystallite size of anatase (nm)
		Si	Ti	organo-silica	TiO_2	
S_N-50	123	-	-	-	-	-
TiO_2/S_N-50	98	63 ± 9	37 ± 9	69	31	-
TiO_2/S_N-400	230	69 ± 12	31 ± 12	66	34	5.5
TiO_2/S_N-600	88	57 ± 7	43 ± 7	50	50	9.4

One of the interesting aspects of this system is the water floatability of the TiO_2/S_N hybrids. Fig. 4 illustrates differences in floatability depending on the presence of organic moieties in TiO_2/S_N samples. ~~While~~ S_N-50, TiO_2/S_N-50, and TiO_2/S_N-400 particles floated on water, while the TiO_2/S_N-600 sample sank.~~–~~ It has been reported that the low density of the

catalyst support is an important factor with respect to the floatability [10,16]. We also deduced that a surface-active effect of the organosilicas at the air–water interface plays a dominant role in the floatability, considering the absence of organic groups in TiO_2/S_N-600. It was reported that surface modification of silica particles with poly(dimethylsiloxane) becomes hydrophobic to afford water-floatable particles [33]. When the TiO_2 nanoparticles were mounted on the porous organosilica supports (S_N-50, and S_N-400), the floatability continued for a longer period (1 week) as exemplified in the Supplementary Data (Fig. S3). Contact angles of TiO_2/S_N-50 and TiO_2/S_N-400 were 129° and 139°, respectively (see the photograph shown in the Supplementary Data, Fig. S3), showing that the surface of these hybrids is water-repellent.

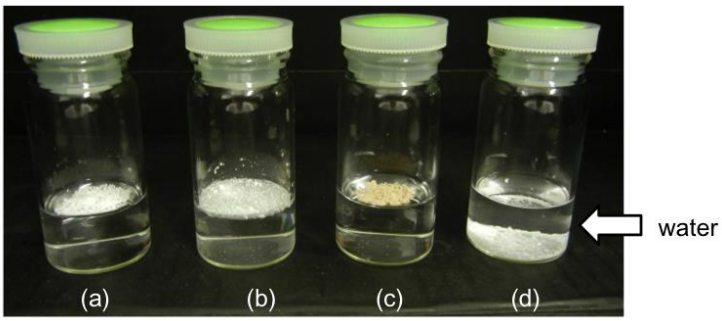

Fig. 4. Photographs of water mixed with (a) S_N-50, (b) TiO_2/S_N-50, (c) TiO_2/S_N-400, and (d) TiO_2/S_N-600.

3.2. Photocatalytic activity

Photo-oxidation of formic acid in O_2-saturated water using a solar simulator was performed to elucidate the photocatalytic activity. Whereas TiO_2/S_N-50 did not decompose formic acid at all, TiO_2/S_N-400 produced CO_2 as shown in Fig. 5, reflecting the high crystallinity of anatase. The relation between the added sample amount and the activity was examined to

elucidate the effect of floatability on photocatalysis. The amount of evolved CO_2 linearly increased with the amount of TiO_2/S_N-400 up to 45 mg, indicating that the cross-sectional light receiving area available to TiO_2/S_N-400 increased with the amount of TiO_2/S_N-400. Further addition of TiO_2/S_N-400 up to 60 mg produced a horizontal plateau, which predicts a maximum light receiving area of approximately 7 cm^2, which is equal to the cross-sectional area of the reaction vessel. In a separate experiment, we estimated that 0.12 g TiO_2/S_N-400 corresponds to filling a water surface with TiO_2/S_N-400 particles in a floating experiment using a 50 mL Pyrex beaker (with a cross-sectional area of 17 cm^2; see the photograph shown in the Supplementary Data, Fig. S43). Since the cross-sectional area of the reaction vessel in the earlier experiment is 7 cm^2, the estimated amount of TiO_2/S_N-400 needed to fill the water surface is 0.05 g, which corresponds to the saturated amount of evolved CO_2. Thus, we empirically demonstrate that floating TiO_2/S_N-400 on water is important for receiving light, and thus, the effective light receiving area is regarded as 1.4×10^2 cm^2/g.

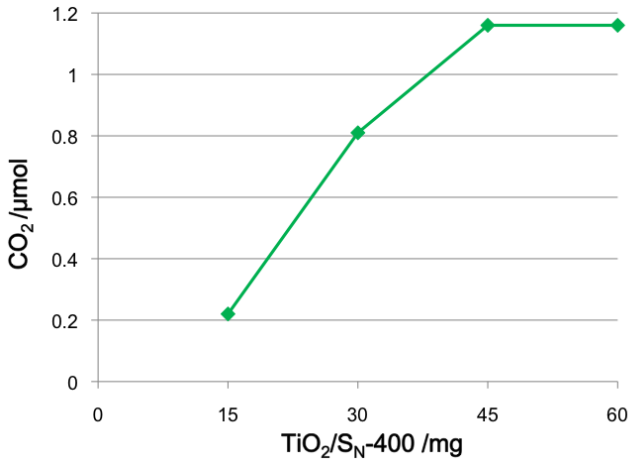

Fig. 5. Photocatalytic CO_2 evolution from aqueous solutions of formic acid on which TiO_2/S_N–400 powders are floated.

4. Conclusion

Organosilica particles incorporating amino groups ~~(S_N-50)~~ were developed as a support for TiO_2 nanoparticles in floating photocatalyst particles~~. The organosilica was fabricated~~ through ~~cooperative~~ hydrolysis and polycondensation ~~reactions~~ of 3-aminopropyltrimethoxysilane, ~~hydrolyzed~~ octyl- and methyl-silyl trichlorides on water droplets in a W/O emulsion, followed by reactions with ~~hydrolyzed 3-aminopropyltrimethoxysilane. Hydrolysis of~~ $TiOSO_4 \cdot xH_2SO_4$ ~~resulted in it becoming favorable for the immobilization of TiO_2 nanoparticles on S_N-50, which was not the case when titanium (IV) tetraisopropoxide was used~~. Amino groups in the organosilica were required to achieve good dispersion of TiO_2 on the surface~~ of the organosilica because phase separation occurred between TiO_2 and organosilica with no amino groups (S_0-50)~~. Acid–base interactions with amino groups are responsible for

TiO_2 hybridization. ~~The resulting hybrid sample, TiO_2/S_N-50, exhibited water-floatability.~~ Floatability on water was maintained ~~shown~~ after calcination at 400 °C ~~in an airflow, resulting in the loss of octyl and 3-aminopropyl groups (TiO_2/S_N-400)~~, whereas ~~floatability~~ was lost after calcination at 600 °C ~~due to oxidative decomposition of all the organic groups (TiO_2/S_N-600)~~. ~~Therefore, organic groups, including methyl groups, in addition to the low density of the particles, play a crucial role in water floatability. Upon using a solar simulator to irradiate floating TiO_2/S_N-400 on an aqueous solution of formic acid, photo-oxidation was observed.~~ The calcination temperature of 400 °C was important in improving the ~~photocatalytic~~ activity of photo-oxidation of formic acid in water, because it increased the specific surface area ~~(to 230 m^2/g)~~ and enhanced the crystallinity of anatase. When the surface of the aqueous solution was filled with the calcined hybrid ~~TiO_2/S_N-400~~ particles, the activity saturated, showing that a "Langmuir monolayer" of the floating ~~TiO_2/S_N-400~~ particles on water efficiently received light. Thus, we empirically demonstrated that the present water-floatable photocatalyst particles efficiently receive light as a result of the careful design of TiO_2 nanoparticles and their organosilica supports through selection of organosilanes, TiO_2 precursors, and calcination temperature.

Appendix A. Supplementary data

Supplementary data associated with this article can be found, in the online version, at http://dx.doi/org/10 .

Acknowledgment

One of the authors (T.O.) acknowledges JSPS (Grant-in-Aid for Scientific Research, #26810121), Cosmetology Research Foundation, and JGC-S Scholarship Foundation.

References

[1] M. Dahi, Y. Liu, Y. Yin,Chem. Rev. 114 (2014) 9853–9889.

[2] S. Anandan , M. Yoon , J. Photochem. Photobiol. C 4 (2003) 5–18.

[3] T. Kamegawa, Y. Ishiguro, H. Seto, H. Yamashita, J. Mater. Chem. A 3 (2015) 2323–2330.

[4] H. Nur, S. Ikeda, B. Ohtani, Chem. Commun. (2000) 2235–2236.

[5] K. M. Choi, S. Ikeda, S. Ishino, K. Ikeue, M. Matsumura, B. Ohtani, Appl. Catal. A: General 278 (2005) 269–274.

[6] K. Ramanathan, D. Avnir, A. Modestoy, O. Lev, Chem. Mater. 9 (1997) 2533–2540.

[7] F. Magalhães, F. C. C. Moura, R. M. Lago, Desalination. 276 (2011) 266–271.

[8] M. E. Fabiyi, R. L. Skelton, J. Photochem. Photobiol. A 132 (2000) 121–128.

[9] F. Magalhães, R. M. Lago, Solar Energy 83 (2009) 1521–1526.

[10] F. Shia, Y. Li, H. Wanga, Q. Zhang, Appl. Catal. B: Environ. 123–124 (2012) 127–133.

[11] L. C. R. Machado, C. B. Torchia, R. M. Lago, Catal. Commun. 7 (2006) 538–541.

[12] M. Dtugosz, J. Was, K. Szczubiatka, M. Nowakowska, J. Mater. Chem. A 2 (2014) 6931–6938.

[13] M. Nair, Z. Luo, A. Heller, Ind. Eng. Chem. Res. 32 (1993) 2318–2323.

[14] P. Huo, Y. Yan, S. Li, H. Li, W. Huang, Appl. Surf. Sci. 256 (2010) 3380–3385.

[15] J. Wang, B. He, X. Z. Kong, Appl. Surf. Sci.327 (2015) 406–412.

[16] C. Shifu, C. Gengyu, Solar Energy. 79 (2005) 1–9.

[17] K. Inumaru, T. Kasahara, M. Yasui, S. Yamanaka, Chem. Commun. (2005) 2131–2133.

[18] T. Ohno, T. Tsubota, K. Kakiuchi, S. Miyayama, K. Sayama, J. Mol. Catal. A: Chem. 245 (2006) 47–54.

[19] F. Caruso, Adv. Mater. 13 (2001) 11–22.

[20] X. W. Lou, L. A. Archer, Z. Yang, Adv. Mater. 21 (2008) 3987–4019.

[21] X. Song, L. Gao, J. Phys. Chem. C 111 (2007) 8180–8187.

[22] S. Mishima, T. Okada, T. Sakai, R. Kiyono, T. Haeiwa, Polym. J. 47 (2015) 449–455.

[23] S. Mishima, M. Kawamura, S. Matsukawa, T. Nakajima, Chem. Lett. 11 (2002) 1092–1093.

[24] T. Okada, K. Miyamoto, T. Sakai, S. Mishima, ACS. Catal. 4 (2014) 73–78.

[25] T. Okada, Y. Takeda, N. Watanabe, T. Haeiwa, T. Sakai, S. Mishima, J. Mater. Chem. A 2 (2014) 5751–5758.

[26] H. Shibata, S. Ohshika, T. Ogura, S. Watanabe, K. Nishio, H. Sakai, M. Abe, K. Hashimoto, M. Matsumoto, J. Photochem. Photobiol. A 217 (2011) 136–140.

[27] K. M. Parida, N. Sahu, A. K. Tripathi, V. S. Kamble. Environ. Sci. Technol. 44 (2014) 4155–4160.

[28] K. M. Parida, B. Naik, J. Colloid Interface Sci. 333 (2009) 269–276.

[29] M. Mureseanu, V. Pârvulescu, R. Ene, N. Coatera, T. D. Pasatoiu, M. Andruh, J. Mater. Sci. 44 (2009) 6795−6804.

[30] H. M. Mody, H. C. Bajaj, Ind. Eng. Chem. Res. 49 (2010) 8184−8191.

[31] Y. Kuroda, T. Mori, K. Yagi, N. Makihara, Y. Kawahara, M. Nagao, S. Kittaka, Langmuir 21 (2005) 8026−8034.

[32] L. Ghindes-Azaria, S. Levy, L. Keinan-Adamsky, G. Goobes, J. Phys. Chem. C 116 (2012) 7442−7449.

[33] K.G. Marinova, D. Christova, S. Tcholakova, E. Efremov, N. D. Denkov, Langmuir 21(2005) 11729−11737.